The Heat of Formation of 2-$C_3H_7^+$ and Proton Affinity of C_3H_6 Determined by Pulsed Field Ionization−Photoelectron Photoion Coincidence Spectroscopy

Tomas Baer*

Department of Chemistry, University of North Carolina, Chapel Hill, North Carolina 27599-3290

Y. Song and C. Y. Ng

Ames Laboratory, U.S. Department of Energy, and Department of Chemistry, Iowa State University, Ames, Iowa 50011

Jianbo Liu and Wenwu Chen

Lawrence Berkeley National Laboratory, Chemical Sciences Division, Berkeley, California 94720

Received: September 13, 1999; In Final Form: December 2, 1999

Pulsed field ionization combined with ion coincidence has been used with synchrotron radiation at the Advance Light Source (ALS) operated in the multibunch mode to energy select ions and to measure their breakdown diagram. The resolution for ion state selection achieved with Ar on this instrument is 0.6 meV. The production of the 2-$C_3H_7^+$ ion was investigated by measuring the dissociative ionization onset from the 2-propyl chloride, bromide, and iodide. Because the dissociation limits for halogen atom loss lie in the Franck−Condon gap, the yield of threshold electrons generated by pulsed field ionization was found to be extremely low. Nevertheless, the heat of formation of 2-$C_3H_7^+$ determined from the three molecules agreed to within 2 kJ/mol. The average and now recommended values for this heat of formation are 825.0 ± 1.5 kJ/mol (0 K) and 807.5 ± 1.5 kJ/mol (298 K). This can be combined with the known heats of formation of C_3H_6 and H^+ to yield a proton affinity of C_3H_6 of 742.3 ± 1.5 kJ/mol (298 K). This new value, which is 9.3 kJ/mol lower than the recommended value of Hunter and Lias, is in much better agreement with two theoretical values (744 kJ/mol) as well as the determination of Szulejko and McMahon (746.4 kJ/mol).

Introduction

The heat of formation of the 2-$C_3H_7^+$ ion is by most measures well established. On the other hand, the heat of formation of this ion serves an essential role in fixing the proton affinity scale[1] through the following reaction:

$$C_3H_6 + H^+ \rightarrow 2\text{-}C_3H_7^+ \quad (1)$$

The gas-phase proton affinity scale has been established over the years by measuring relative proton affinities through either bracketing[2,3] or equilibrium studies in high-pressure mass spectrometers.[4−6] This relative scale is fixed or anchored at several points by ions whose heats of formation can be established by well characterized methods. Among these methods is that of dissociative photoionization which in the case of 2-$C_3H_7^+$ involves the dissociation of 2-$C_3H_7X^+$ ions, where X = Cl, Br, I, or H. Other ions, which serve a similar function in different parts of the proton affinity scale are the heats of formation of $C_2H_5^+$, $C_4H_9^+$, HCO^+, and $(CH_3)COH(CH_3)^+$.[1,6] These ions have in common the property that their saturated precursors lose an atom or molecular group and produce an ion which is identical to the attachment of a proton to an unsaturated molecule.

There is currently considerable disagreement concerning the 298 K proton affinity of C_3H_6. At one extreme, Hunter and Lias[1] list a value of 751.6 kJ/mol which is based primarily on the 2-$C_3H_7^+$ heat for formation reported by Rosenstock et al.,[7] while two high-level theoretical studies suggest a value of 744 kJ/mol.[8,9] Between are other experimental values such as 746.4 ± 2 kJ/mol[6] and 748 ± 2 kJ/mol.[10−12]

In the case of 2-$C_3H_7^+$, the useful saturated precursors and their dissociative ionization reactions that lead to the 2-$C_3H_7^+$ ion are the following:

$$2\text{-}C_3H_7Cl + h\nu \rightarrow 2\text{-}C_3H_7^+ + Cl + e^- \quad (2)$$

$$2\text{-}C_3H_7Br + h\nu \rightarrow 2\text{-}C_3H_7^+ + Br + e^- \quad (3)$$

$$2\text{-}C_3H_7I + h\nu \rightarrow 2\text{-}C_3H_7^+ + I + e^- \quad (4)$$

$$C_3H_8 + h\nu \rightarrow 2\text{-}C_3H_7^+ + H + e^- \quad (5)$$

There are of course other reactions that lead to the 2-$C_3H_7^+$ ions, such as CH_3 loss from iso-$C_4H_{10}^+$. However, this is not the lowest energy channel (CH_4 and H loss[13] have lower dissociation energies) so that the accurate determination of the onset for 2-$C_3H_7^+$ formation is made difficult by the fact that this channel must compete with the other channels. To our knowledge, the above four reactions are the only ones having the following essential features: (a) the lowest energy dissociation channels produce the ion of interest; (b) the reactions do not appear to involve barriers in the dissociation channel;[7] (c) the reactions are sufficiently rapid so that products are formed on the time scale of the experimental mass analysis; (d) the

* Corresponding author.

10.1021/jp993244i CCC: $19.00
Published on Web 02/02/2000

heats of formation of the precursor molecules, 2-C_3H_7X, are reasonably well established. The absence of any one of these properties eliminates a candidate molecule from consideration.

The determination of dissociation onsets presents a number of difficulties. Among the accurate approaches involving photoionization, the historically first method and one still used today is the measurement of the onset for product formation of the fragment ion.[14−16] Because most experiments are carried out with thermal samples, this approach must take into account the fact that the high-energy tail of the internal energy distribution leads to a similar tail in the measured onset. Through careful analysis which takes into account the photoelectron deposition function and the thermal energy distribution, it is possible to be somewhat more certain than simply choosing the onset at the energy at which the fragment ion signal is lost in the noise.[17−19] In principle, the use of cooled molecules in a supersonic expansion should improve the situation. However, the combination of an imperfect and largely unknown cooling efficiency[20] and the inevitable thermal background in the photoionization chamber makes this approach less than ideal.

We have recently developed a high-resolution photoelectron photoion coincidence (PEPICO) method which is based on pulsed field ionization (PFI) of high-n ($n > 100$) Rydberg states.[21] This experiment has the capability of selecting the ions with submillivolt resolution and thus to provide us with a very precise measure of the dissociative ionization onset for the above-mentioned reactions. This is almost an order of magnitude improvement in the resolution of the ion energy compared to previous threshold PEPICO experiments. On the other hand, the signal level in PFI−PEPICO for certain molecular systems, such as our $C_3H_7X^+$ ions, is found to be very low (in part due to the high resolution), so that the full advantage of this approach is not realized in this study.

Previous studies of the 2-$C_3H_7^+$ heat of formation have been based on the dissociative ionization onset of halogen atom loss from 2-$C_3H_7Br^+$ and 2-$C_3H_7I^+$ using the threshold PEPICO method,[7] and these same precursors plus 2-$C_3H_7Cl^+$ in a photoionization study.[11] We have repeated these measurements and have paid special attention to Cl loss from the 2-$C_3H_7Cl^+$ ion. The latter has the advantage that the heat of formation of the neutral precursor is known more accurately than that of the bromine and iodine analogues, so that it should potentially provide us with the most accurate value for the heat of formation of the 2-$C_3H_7^+$ ion.

Experimental Approach

The experimental arrangement and procedures for PFI-photoelectron spectroscopy[22,23] and the recent extension to PFI−PEPICO measurements have been thoroughly discussed by Jarvis et al.[21] and so we will only outline the basic principles of the technique. Synchrotron radiation from an undulator is dispersed by a 6.5 m monochromator. The ring, operated in the multibunch mode, generates 512 ns of quasicontinuous radiation followed by a 144 ns dark gap. The photons excite the molecular beam cooled sample in the presence of an 0.2 V/cm electric field to energies in the vicinity of the dissociative ionization threshold. While the promptly produced electrons and ions are extracted by the small dc field, neutrals in high-n Rydberg states remain in the ion source. They are stabilized by the low dc, or stray electric fields through Stark mixing of the l and m_l states.[24] These high-n and l Rydberg states are then field ionized during the 144 ns dark gap by a 7 V/cm, 200 ns long pulsed electric field. The PFI electrons are collected in a 5 ns window which serves to discriminate against all nonfield-ionized electrons that are produced by direct ionization. The success of this experiment is due in large part to the very high photon resolution (<0.001 eV) of the 6.5 m monochromator[25] which permits excitation of the narrow band of high-n Rydberg states.

The ions are extracted by the constant dc field of 0.2 V/cm as well as by the 1.52 MHz, 7 V/cm pulsed field. The parent 2-$C_3H_7Cl^+$ parent ions spend about 6 μs in the pulsed 6 mm acceleration region, while the product $C_3H_7^+$ daughter ions spend 4.5 μs there. Thus, they require on the average nine and seven pulsing cycles to exit this first acceleration region. The heavier bromo- and iodopropane ions require correspondingly more cycles to exit the region. The average electric field in this quasicontinuous acceleration region is about 3 V/cm. Typical collection efficiencies for Ar at its ionization energy were 6% for PFI electrons and 30% for ions.

The PFI electrons provided the start signal for a Stanford Research Systems multichannel scaler with a maximum resolution of 5 ns. The ion TOF resolution used in this study was 40 ns per channel. Time-of-flight spectra were collected at fixed photon energies. The PFI signal rates were not high because the interesting dissociation regions in all three ions are located in Franck−Condon gaps. In addition, the high-energy resolution necessarily reduces the number of electrons within the narrow energy window. Typical count rates were 1−10 c/s PFI electrons, 2000−20 000 c/s ions, and 0.1−1 coincidence events per second. Most ion TOF distributions were collected over a period of 1−2 h. All ions were collected with no suppression of "false" ions. It was necessary in many cases to close the slits in order to keep the total ion count rates down to avoid the build up of a false coincidence background. Two planned modifications may improve the signal-to-noise ratio in future experiments. One is the installation of a fast ion gate which will permit only ions associated with a PFI electron to be collected, thereby dramatically reducing the false coincidence counts, and the other is the installation of a time varying field[26] which may help stabilize the high-n Rydberg states.

All three samples have vapor pressures that are below atmospheric pressure, and so the samples were seeded in a molecular beam of Ar. Argon was chosen in part because it provides for cooling without giving the sample too high a velocity perpendicular to the ion extraction field. Argon was passed at a pressure of about 1 atm over a liquid sample of 2-C_3H_7X, X = Cl, Br, or I. Upon ionization, the ions were accelerated to a final energy of 120 eV through three acceleration regions, and traveled with this energy through the 40 cm long drift tube where they were detected by a set of microchannel plates. The translational temperature of the molecular beam as measured from the TOF peak widths was about 30 K. However, as will be discussed, this is not necessarily a good measure of the internal energy of the molecules in the beam.[20]

Results and Discussion

a. The Breakdown Diagrams. Figure 1 shows some typical PFI−PEPICO TOF spectra of 2-$C_3H_7Cl^+$ and 2-$C_3H_7^+$ ions at various photon energies near the dissociation onset. Similar TOF spectra were obtained at other photon energies. The net parent and daughter ion areas were obtained by subtracting the false coincidence background from the total signal. Because the extraction is quasicontinuous, the false coincidence background signal is essentially flat. The parent and daughter ion peak areas in Figure 1 were divided by the total parent and daughter ion signal and plotted as a function of the photon energy. This breakdown diagram is shown in Figure 2. It shows that at low energies, only the parent ion is stable, but that, as the dissociation

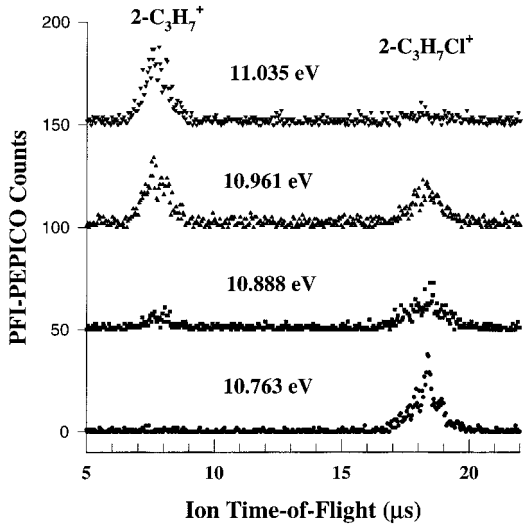

Figure 1. PFI−PEPICO time-of-flight distributions for 2-C_3H_7Cl at selected photon energies. The peak shapes do not have the Gaussian form because the ions are extracted by a train of 8V/cm pulses with an average field of about 3 V/cm.

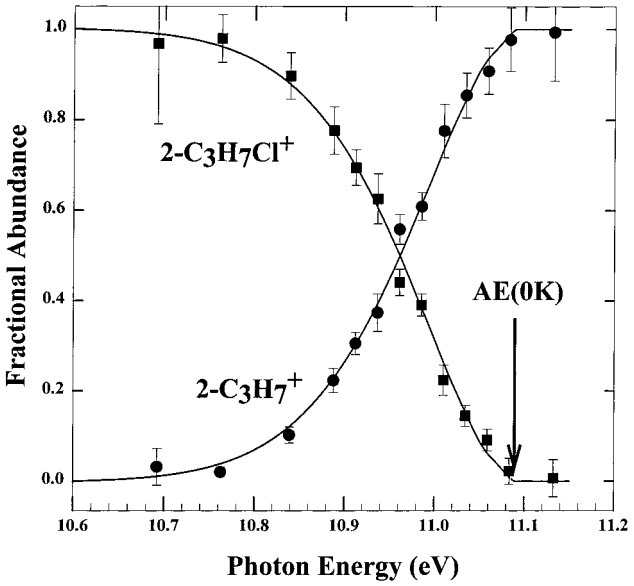

Figure 2. Breakdown diagram for 2-$C_3H_7Cl^+$ in the vicinity of the Cl loss dissociation limit. The 0 K dissociation limit is indicated by the vertical arrow.

onset is approached, the fraction of parent ions slowly diminishes, until it reaches zero at 11.085 eV. The error bars, which represent the standard deviation of each point, were determined by assuming that the error in the number of counts, N, is given by $\sqrt{N}$. Thus, the false coincidence background signal contributed to the error at each point.

The breakdown diagram was fitted by assuming that the ion energy resolution is infinitely narrow and that the broadening of the breakdown diagram is due solely to the thermal energy in the 2-C_3H_7Cl molecule. The thermal energy distribution in 2-C_3H_7Cl was determined by calculating the density of the rovibrational states ($\rho(E)$) and using this to obtain the distribution of internal energy, $P(E)$.

$$P(E) = \frac{\rho(E)\, e^{-E/RT}}{\int_0^\infty \rho(E)\, e^{-E/RT}} \qquad (6)$$

The density of states were calculated with vibrational frequencies determined by ab initio molecular orbital calculations (HF 6-31G* basis sets) and scaled according to Pople et al.[27] The solid lines in Figure 2 were obtained by convoluting this thermal energy distribution with a step function at the dissociation limit (AE) as given by eqs 7 and 8,

$$\text{parent}(h\nu) = \int_0^{\text{AE-}h\nu \text{ or } 0} P(E)\, dE \qquad (7)$$

$$\text{daughter}(h\nu) = \int_{\text{AE-}h\nu \text{ or } 0}^{\infty} P(E)\, dE \qquad (8)$$

where the integration limits are either AE-hν or 0, whichever is greater. This assumes that all ions with energies in excess of the dissociation limit fragment within 1 μs. A fast dissociation is consistent with the statistical theory of unimolecular dissociation (RRKM).[28] The data were fitted by varying both the temperature of the sample as well as the 0 K AE. These two parameters are quite independent of each other. The AE shifts the calculated breakdown diagram along the energy axis, while the temperature determines the slope at which the parent ion signal disappears at the 0 K appearance energy. This AE(0 K) is shown by the arrow in Figure 2. In the case of the 2-propylchloride data, a temperature of 350 K gave the best fit for the data.

It might appear strange that the breakdown diagram was fitted with an assumed temperature of 350 K when the sample clearly has a temperature below that of room temperature. A full understanding of this is not yet in hand. However, the basic idea is as follows. Experiments on the dissociation dynamics of CH_4^+ showed that, in PFI, the efficiency of producing electrons by PFI seems to depend on whether the Rydberg state remains intact or it dissociates.[29] This was made very evident by the fact that the yield of PFI electrons abruptly increased at the dissociation limit of CH_4. A similar effect was observed for H_2O^+ a number of years ago by Stockbauer[30] and confirmed by Dutuit et al.,[31] although in those studies, the detected electrons were threshold electrons and not electrons generated by delayed pulsed field ionization. The net result is an increased yield of PFI electrons from fragments over those from parents. This has the effect of increasing the fragment ion signal relative to the parent ion signal. Although the breakdown diagram could be modeled by including an adjustable factor that takes this into account, adjusting the temperature is just as convenient and seems no more arbitrary.

The important point is that the information of interest, which is the 0 K dissociation limit (AE), is independent of how the breakdown diagram is fitted. This 0 K limit is the point in the breakdown diagram at which the parent ion signal disappears.[29] If the sample temperature were 0 K and in the absence of thermal background gas in the chamber, the breakdown diagram would consist of vertical lines at the 0 K onset. Thus, the only effect of the thermal sample is to change the slope at which this onset is approached. The derived 0 K onset for 2-$C_3H_7^+$ ions from 2-C_3H_7Cl is 11.085 ± 0.005 eV. This onset energy is determined by both the disappearance of the parent ion signal and the fitting of the breakdown diagram between 10.9 and 11.1 eV.

Figures 3 and 4 show similar breakdown diagrams for the case of 2-C_3H_7Br and 2-C_3H_7I. Because of the weaker PFI signal for the 2-C_3H_7Br and 2-C_3H_7I compounds, the error bars for each point and the experimental uncertainty of the whole breakdown diagram are somewhat greater for those compounds than they are for the 2-C_3H_7Cl data. In addition, for both the 2-C_3H_7Br and the 2-C_3H_7I data, the PFI signal contained some hot or scattered electrons whose importance became more

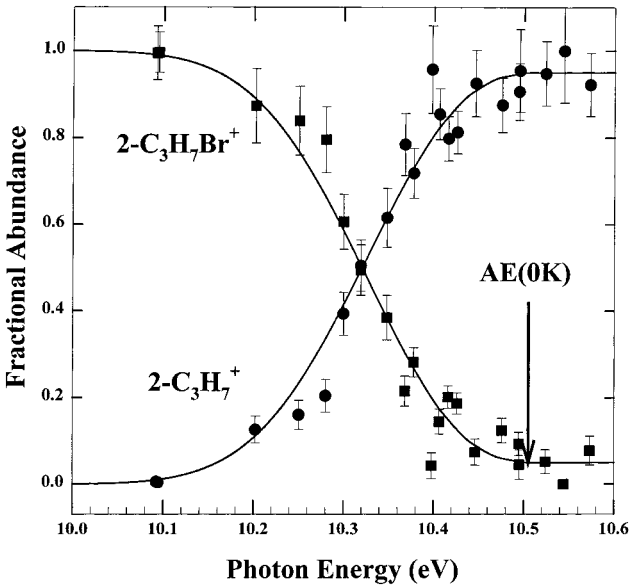

Figure 3. breakdown diagram for 2-$C_3H_7Br^+$ in the vicinity of the Br loss dissociation limit. The 0 K dissociation limit is indicated by the vertical arrow.

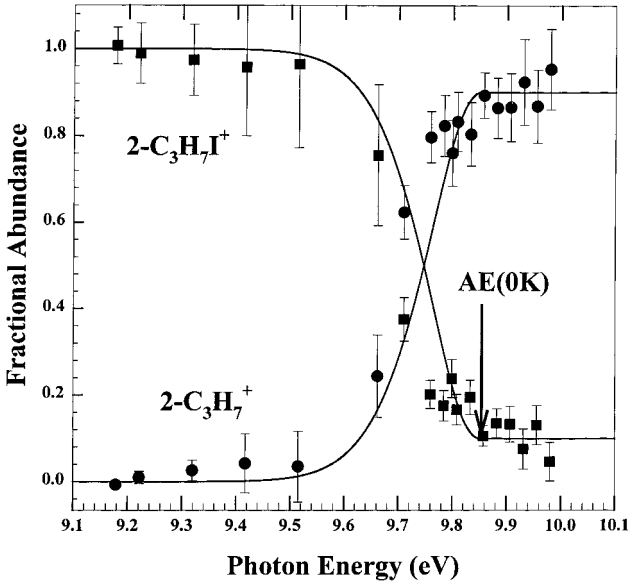

Figure 4. Breakdown diagram for 2-$C_3H_7I^+$ in the vicinity of the I loss dissociation limit. The 0 K dissociation limit is indicated by the vertical arrow.

evident in light of the weak real PFI signal. Such signal is difficult to avoid when the PFI signal rate is on the order of 1 c/s. A noise of 0.1 c/s on the electron detector can result in a significant parent ion signal, the intensity of which depends on the total ionization rate. As a result, the parent ions never disappeared completely above the 0 K dissociation limit. The data were thus modeled by normalizing to 5% and 10% background signal for the propyl bromide and propyl iodide parent ions, respectively.

The primary experimental data obtained from this study are the 0 K dissociation onsets which can be compared to onsets from similar studies by other groups. The numbers obtained by photoionization experiments are shown in Table 1. It is curious that our onsets are larger than the Rosenstock[7] values for 2-C_3H_7-Br and 2-C_3H_7I. Those breakdown diagrams were analyzed in a manner similar to the present ones and in principle should have yielded the same onsets. The major difference in the two

TABLE 1: Dissociative Photoionization Onsets (in eV) Obtained for 2-C_3H_7X Molecules

molecule	0 K onset	method
2-C_3H_7Cl	11.085 ± 0.005	PFI−PEPICO (this work)
	$11.03^a \pm 0.01$	PIE (Traeger[11])
2-C_3H_7Br	10.505 ± 0.020	PFI PEPICO (this work)
	10.42 ± 0.01	TPEPICO (Rosenstock et al.[7])
	$10.44^b \pm 0.01$	PIE (Traeger[11])
2-C_3H_7I	9.851 ± 0.025	PFI−PEPICO (this work)
	9.77 ± 0.02	TPEPICO (Rosenstock et al.[7])
	$9.82^c \pm 0.01$	PIE (Traeger[11])

[a] Obtained by adding the average thermal energy of 0.107 eV to reported 298 K onset. [b] Obtained by adding the average thermal energy of 0.112 eV to reported 298 K onset. [c] Obtained by adding the average thermal energy of 0.117 eV to reported 298 K onset.

TABLE 2: Heats of Formation in kJ/mol of Neutral Precursors and Products

molecule	$\Delta_f H°_{298K}$	$\Delta_f H°_{0K}$	$H°_{298} - H°_0$
2-C_3H_7Cl	-144.9 ± 1.3^a	-124.0 ± 1.3^b	16.5^b
2-C_3H_7Br	-99.4 ± 2.5^a	-71.3 ± 2.5^b	17.0^b
2-C_3H_7I	-40.3 ± 3.8^a	-18.4 ± 3.8^b	17.5^b
C_3H_6	20.0 ± 0.8^a	35.3^c	13.3^c
Cl	121.3^d	119.6^d	6.27^d
Br	111.9^d	117.9^d	6.20^d
I	106.8^d	107.2^d	6.20^d

[a] From Pedley et al.[38] [b] Derived using calculated (HF6-31G* level) C_3H_7X vibrational frequencies scaled by 0.893. [c] Calculated using vibrational frequencies from Herzberg.[42] [d] From Wagman et al.[39] and Cox et al.[43]

experiments is in the resolution of the ion internal energy which in our case was about 2 meV while their resolution function has a full width at half-maximum (fwhm) of 27 meV and contains a long hot electron "tail". Thus, errors associated in fitting their breakdown diagram are more easily introduced.

Rosenstock et al.[7] reported some unusual features in their experimental results. They observed a slight shift in the appearance energy in their delayed ion extraction scheme which is characteristic of a slow dissociation. Yet, as noted by them, the statistical RRKM theory indicates that this reaction should not be slow, nor did our PEPICO results suggest such a slow dissociation. Slow dissociations result in asymmetric fragment ion TOF distributions.[32] The present PFI−PEPICO data as well as previous PEPICO results on 2-C_3H_7I,[33] indicated that the TOF distributions are symmetric. This unexplained shift with pulse delay in the Rosenstock breakdown diagram may be related to the discrepancy between their onsets and ours.

Our results are in somewhat better agreement with those of Traeger[11] although the discrepancy of 0.055 eV for the case of the 2-propyl chloride data is far beyond the limits of the claimed accuracy of both methods. We have no explanation for this difference.

b. The 2-$C_3H_7^+$ Ion Heat of Formation. The conversion of the measured onsets into a 2-$C_3H_7^+$ heat of formation assumes that there is no reverse activation barrier, and that the ion dissociation is fast. In addition, the derived heat of formation is based on auxiliary heats of formation for the precursor 2-C_3H_7X molecules and X atoms. The auxiliary heats of formation used here are listed in Table 2. It is important to note that, of the three molecules, the isopropyl chloride heat of formation is the most accurately known. In the Rosenstock study, the somewhat lower $\Delta_f H°_{0K}$ values for 2-C_3H_7I of −20.1 kJ/mol was used. Thus, the lower measured dissociative photoionization onset, plus a lower assumed heat of formation for the starting material, both conspire to reduce the derived 2-$C_3H_7^+$ heat of formation from the propyl iodide data relative

TABLE 3: Derived Heats of Formation in kJ/mol of the 2-$C_3H_7^+$ Ion[a]

$\Delta_fH°_{0K}$	$\Delta_fH°_{298K}$	source
825.9 ± 1.3	808.6 ± 1.3	PFI−PEPICO 2-C_3H_7Cl (this work)
824.4 ± 2.5	807.1 ± 2.5	PFI−PEPICO 2-C_3H_7Br (this work)
824.9 ± 3.8	807.6 ± 3.8	PFI−PEPICO 2-C_3H_7I (this work)
825.0 ± 1.5	807.7 ± 1.5	average of present PFI−PEPICO results
816.2 ± 2	798.9 ± 2	PEPICO 2-C_3H_7Br (Rosenstock et al.[7]) recalculated[b]
817.1 ± 4	799.8 ± 4	PEPICO 2-C_3H_7I (Rosenstock et al.[7]) recalculated[b]
820.2	802.9	PIE of 2-C_3H_7Cl Traeger et al.[10−12]
818.2	800.9	PIE of 2-C_3H_7Br Traeger et al.[10−12]
821.6	804.3	PIE of 2-C_3H_7I Traeger et al.[10−12]
819.9	802.6	PIE of C_3H_8 (Chupka and Berkowitz[44]) recalculated[c]

[a] The 0 K electron energy convention is used here for the 298 K value. If the electron is assumed to have an energy of 5/2*RT* at 298 K, then 6.2 kJ/mol must be added to the 298 K heat of formation in the case of ions, such as 2-$C_3H_7^+$ (see Lias et al.[34]). $H°_{298}-H°_0(C_3H_7^+)$ is taken as 15.45 kJ/mol (Smith and Radom[9]). [b] These heats were recalculated using the auxiliary heats of formation listed in Table 2. See also Traeger and Kompe.[12] [c] This heat of formation was calculated from the Chupka and Berkowitz 0 K onset for H loss from C_3H_8 of 11.59 eV and the $\Delta_fH°_{0K}(C_3H_8) = -82.4$ kJ/mol and $\Delta_fH°_{0K}(H) = 216$ kJ/mol.[39] See also Traeger and Kompe.[12]

TABLE 4: Derived Proton Affinities (kJ/mol) for C_3H_6 from Various Sources

PA(0 K)	PA(298 K)	source
738.3 ± 1.5	742.3 ± 1.5	PFI−PEPICO this study
	751.4 ± 2.9	T-PEPICO study by Rosenstock et al.[7]
	751.6	Hunter and Lias[1], a primary standard
	746.4 ± 2.0	Szulejko and McMahon[6] measured by proton-transfer equilibria relative to the PA(CO)
	747.7 ± 2	PIE study by Traeger and McLoughlin[10]
740.3	744.3	Smith and Radom[9] a calculated value
	744	Koch et al.[8] a calculated value

to our value. Our values for the heat of formation of 2-$C_3H_7^+$ along with those of other workers are shown in Table 3.

The derived 2-$C_3H_7^+$ heats of formation are on the high side compared to previous measurements. However, they agree very well with each other. Because of the quality of the breakdown diagram in Figure 1, and the precision of the neutral 2-C_3H_7Cl heat of formation, we tend to favor the results from this molecule. We thus propose an average $\Delta_fH°_{0K}$ value of 825.0 ± 1.5 kJ/mol and a $\Delta_fH°_{298K}$ of 807.7 ± 1.5 kJ/mol to which we assign a precision similar to the error limits associated with the propyl chloride data.

c. The Proton Affinity of C_3H_6 and the Proton Affinity Scale. The 2-$C_3H_7^+$ heat of formation can be converted to a proton affinity (PA) of C_3H_6 using eq 1 which yields

$$PA(C_3H_6) = -\Delta_fH°(2\text{-}C_3H_7^+) + \Delta_fH°(H^+) + \Delta_fH°(C_3H_6) \quad (9)$$

at both 0 K and 298 K. Using the known heats of formation of H^+, 1528.0 kJ/mol (0 K) and 1530.0 kJ/mol (at 298 K),[34] and the values for C_3H_6 listed in Table 2, we derive the proton affinities shown in Table 4. Note that unlike the heats of formation of ions, the proton affinities at 298 K are the same for the 0 K and the 298 K electron convention.

It is clear from Table 4 that there are some major discrepancies in the derived proton affinity of the C_3H_6 molecule. Our value for $PA_{298K} = 742.3 \pm 1.5$ kJ/mol is the lowest one in the list, while the currently "accepted" value of 751.6 kJ/mol is the highest. Between these two extremes is the Traeger value of 747.2 ± 2 kJ/mol. Because of the key role that this molecule plays in establishing the proton affinity scale it is important to determine the origin of this discrepancy and the consequences of using a new value that is 9.3 kJ/mol lower than the "accepted" value in the recent Hunter/Lias compilation.[1,35]

The value of 751.6 kJ/mol in the Hunter and Lias compilation was a value chosen by them based on the available data for the heats of formation of the 2-$C_3H_7^+$ ion. Thus, it is not a value that they derived from their data. They relied heavily on the Rosenstock[7] value. In contrast to this, we have the Szulejko and McMahon value of 746.4 ± 2 kJ/mol which is based on 80 equilibrium measurements between 48 different molecules with proton affinities ranging from 934.7 kJ/mol ($(CH_3)_3CNH_2$) to 496.6 kJ/mol (N_2). The whole scale is anchored to a single value, which is the 298 K proton affinity of CO of 593.7 kJ/mol. This value can be derived from the heat of formation of HCO^+. The latter value has been reported from the dissociative photoionization onset for H loss from the formaldehyde ion,[36] and from the onset for OH loss from formic acid ions.[16] Neither molecule is ideal for determining the HCO^+ heat of formation. The heat of formation of the formaldehyde molecule is not well established. In the most recent compilation, Chase lists the $\Delta_fH°_{298K}(H_2CO)$ as −115.9 ± 6.3 kJ/mol.[37] The data from which this is derived are all prior to 1965. On the other hand, Pedley et al.[38] list a value of −108.6 ± 0.5 kJ/mol, while Wagman et al.[39] list it as −108.57 kJ/mol (with no error bars). None of the data on which this is based appear to be newer than about 1959. Another complication with using formaldehyde as a basis for determining the HCO^+ heat for formation is that H loss reactions often are associated with a centrifugal barrier so that the onset is only an upper limit. The 0 K heat of formation of the HCO^+ ion based on the Guyon et al.[36] onset is thus 829.4 or 822.0 kJ/mol depending on whether the Pedley/Wagman or the Chase heat of formation of H_2CO is used. This leads to a 298 K PA(CO) of 590.7 or 598.1 kJ/mol for the Pedley/Wagman and the Chase data, respectively. These values are on either side of the value chosen as the anchor (593.7 kJ/mol) by Szulejko and McMahon.[6]

The OH loss reaction from formic acid ions is the second dissociation channel (the first is H loss which appears 0.4 eV below the OH loss) so that it is subject to a competitive kinetic shift. On the other hand, the onset is very sharp, which suggests that there is no effect of a kinetic shift, and the heat of formation of formic acid is well established. The Traeger study of formic acid leads to a $\Delta_fH°_{0K}(HCO^+) = 825.8 \pm 2.7$ kJ/mol and thus to a $PA_{298K}(CO)$ of 594 ± 3 kJ/mol.[16] Although the agreement between the photoionization experimental values (primarily due to the uncertain heat of formation of H_2CO) is less than desirable, the proton affinity of CO is also based on the ionization energy of the HCO radial measured as well as ab initio calculations.[6] These results are in agreement with the Traeger value of 594 ± 3 kJ/mol for the proton affinity of CO. It is thus a very reasonable choice for anchoring the proton affinity scale.

There have been several theoretical studies of the heat of formation of 2-$C_3H_7^+$ ion, and the related proton affinity of C_3H_6.[8,9,40,41] The heat of formation is best obtained from the PA by calculating the difference in the energy between $C_3H_6 + H^+$ and 2-$C_3H_7^+$ and referencing the energy scale to the sum of $\Delta_fH°(C_3H_6)$ and $\Delta_fH°(H^+)$, both of which are well established. Koch et al.[8] calculated the energy and structures of a number of 2-$C_3H_7^+$ isomers obtaining optimized structures and vibrational frequencies at the MP2/6-311G** level and calculat-

ing energy differences at the MP4/6-311G** level with the frozen core approximation. They found that the 298 K PA(propene) = 743.9 kJ/mol.

Some years later, Smith and Radom[9,40] used the G2 theory to obtain the PAs of over 30 molecules, including C_3H_6. They found that the 298 K PA(C_3H_6) = 744.3 kJ/mol. The same group investigated the PA values at several levels of theory including MP2, MP4, and density functional theory with several functionals.[40,41] They again found that the best ab initio schemes gave consistent PA values for C_3H_6 which lie between 742 and 744 kJ/mol.

Aside from the Rosenstock measurement, all other experimental and theoretical studies indicate that the PA(C_3H_6) should be lowered relative to the Hunter−Lias compilation. The question is only how much. A simple average of the five values listed in Table 4 yields a $PA_{298K}(C_3H_6)$ of 745 ± 2 kJ/mol, a value that is some 6 kJ/mol lower than the Hunter−Lias number. On the other hand, if we take our value, then the $PA_{298K}(C_3H_6)$ should be 742.3 ± 1.5 kJ/mol.

Conclusion

This PFI−PEPICO study of the 0 K 2-$C_3H_7^+$ onsets from three isopropyl halide molecules has shown that the heat of formation of the 2-$C_3H_7^+$ ion should be adjusted up to 825.0 ± 1.5 (0 K) and 807.7 ± 1.5 kJ/mol (298 K). This is substantially higher than previous values, but is consistent with several values of the related proton affinity of C_3H_6. The proton affinity, based on our results alone, should be reduced to 742 ± 1.5 kJ/mol. If the average of recent experimental and theoretical values is used, the PA(C_3H_6) would be 745 ± 2 kJ/mol. Either value is substantially lower than the Hunter−Lias value of 751.6 kJ/mol.

Acknowledgment. This work was supported by the Chemical Sciences Division of the U.S. Department of Energy Contracts DE-AC03-76SF00098 and DE-FG02-97ER14776. We also thank John Traeger for reading this manuscript prior to publication and for his very helpful comments and suggestions.

References and Notes

(1) Hunter, E. P. L.; Lias, S. G. *J. Phys. Chem. Ref. Data* **1998**, *27*, 413−656.
(2) Bohme, D. K.; Mackay, G. I.; Schif, H. I. *J. Chem. Phys.* **1980**, *73*, 4976−4986.
(3) Sieck, L. W. *J. Phys. Chem. A* **1997**, *101*, 8140−8145.
(4) Mautner, M.; Sieck, L. W. *J. Am. Chem. Soc.* **1991**, *113*, 4448−4460.
(5) Szulejko, J. E.; McMahon, T. B. *Int. J. Mass Spectrom. Ion. Proc.* **1991**, *109*, 279−294.
(6) Szulejko, J. E.; McMahon, T. B. *J. Am. Chem. Soc.* **1993**, *115*, 7839−7848.
(7) Rosenstock, H. M.; Buff, R.; Ferreira, M. A. A.; Lias, S. G.; Parr, A. C.; Stockbauer, R.; Holmes, J. L. *J. Am. Chem. Soc.* **1982**, *104*, 2337−2345.
(8) Koch, W.; Liu, B.; Schleyer, P. v. R. *J. Am. Chem. Soc.* **1989**, *111*, 3479−3480.
(9) Smith, B. J.; Radom, L. *J. Am. Chem. Soc.* **1993**, *115*, 4885−4888.
(10) Traeger, J. C.; McLoughlin, R. G. *J. Am. Chem. Soc.* **1981**, *103*, 3647−3652.
(11) Traeger, J. C. *Int. J. Mass Spectrom. Ion. Phys.* **1980**, *32*, 309−319.
(12) Traeger, J. C.; Kompe, B. M. In *Energetics of Organic Free Radicals*; Martinho Simoes, J. A., Greenberg, A., Liebman, J. F., Eds.; Chapman & Hall: London, 1996; pp 59−109.
(13) Traeger, J. C. *Rapid Comm. Mass. Spectrosc.* **1996**, *10*, 119−122.
(14) Ng, C. Y. *Adv. Chem. Phys.* **1983**, *52*, 263−362.
(15) Steiner, B. W.; Giese, C. F.; Inghram, M. G. *J. Chem. Phys.* **1961**, *34*, 189−220.
(16) Traeger, J. C. *Int. J. Mass Spectrom. Ion. Proc.* **1985**, *66*, 271−282.
(17) Guyon, P. M.; Berkowitz, J. *J. Chem. Phys.* **1971**, *54*, 1815−1826.
(18) Ruscic, B.; Berkowitz, J. *J. Chem. Phys.* **1994**, *101*, 7975−7989.
(19) Werner, A. S.; Tsai, B. P.; Baer, T. *J. Chem. Phys.* **1974**, *60*, 3650−3657.
(20) Mayer, P. M.; Baer, T. *Int. J. Mass Spectrom. Ion. Proc.* **1996**, *156*, 133−139.
(21) Jarvis, G. K.; Weitzel, K. M.; Malow, M.; Baer, T.; Song, Y.; Ng, C. Y. *Rev. Sci. Instrum.* **1999**, *70*, 3892−3906.
(22) Hsu, C. W.; Evans, M.; Ng, C. Y.; Heimann, P. *Rev. Sci. Instrum.* **1997**, *68*, 1694−1702.
(23) Jarvis, G. K.; Song, Y.; Ng, C. Y. *Rev. Sci. Instrum.* **1999**, *70*, 2615−2621.
(24) Chupka, W. A. *J. Chem. Phys.* **1993**, *98*, 4520−4530.
(25) Heimann, P.; Koike, K.; Hsu, C.-W.; Evans, M.; Lu, K. T.; Ng, C. Y.; Suits, A. G.; Lee, Y. T. *Rev. Sci. Instrum.* **1997**, *68*, 1945−1955.
(26) Jones, R. R.; Fu, P.; Gallagher, T. F. *J. Chem. Phys.* **1997**, *106*, 3578−3581.
(27) Pople, J. A.; Scott, A. P.; Wong, M. W.; Radom, L. *Isr. J. Chem.* **1993**, *33*, 345−350.
(28) Baer, T.; Hase, W. L. *Unimolecular Reaction Dynamics: Theory and Experiments*; Oxford University Press: New York, 1996.
(29) Weitzel, K. M.; Malow, M.; Jarvis, G. K.; Baer, T.; Song, Y.; Ng, C. Y. *J. Chem. Phys.* **1999**, *111*, 8267−8270.
(30) Stockbauer, R. *J. Chem. Phys.* **1980**, *72*, 5277−5279.
(31) Dutuit, O. In *Fundamentals of Gas-Phase Ion Chemistry*; Jennings, K. R., Ed.; Kluwer Acad. Publ.: Netherlands, 1991; pp 21−54.
(32) Baer, T.; Booze, J. A.; Weitzel, K. M. In *Vacuum ultraviolet photoionization and photodissociation of molecules and clusters*; Ng, C. Y., Ed.; World Scientific: Singapore, 1991; pp 259−298.
(33) Brand, W. A.; Baer, T.; Klots, C. E. *Chem. Phys.* **1983**, *76*, 111−120.
(34) Lias, S. G.; Bartmess, J. E.; Liebman, J. F.; Holmes, J. L.; Levin, R. D.; Mallard, W. G. Gas-Phase Ion and Neutral Thermochemistry. *J. Phys. Chem. Ref. Data* **1988**, *17* (Suppl. 1).
(35) Hunter, E. P.; Lias, S. G. *Proton Affinity Evaluations in NIST Chemistry WebBook: NIST Standard Reference Databas 69*; Nat. Inst. Standards and Tech (http://webbook.nist.gov): Gaithersburg, MD, 1998.
(36) Guyon, P. M.; Chupka, W. A.; Berkowitz, J. *J. Chem. Phys.* **1976**, *64*, 1419−1436.
(37) Chase, M. W., Jr. *NIST-JANAF Thermochemical Tables*; NIST: Gaithersburg, MD, 1998; pp 1−1951.
(38) Pedley, J. B.; Naylor, R. D.; Kirby, S. P. *Thermochemical Data of Organic Compounds*; Chapman and Hall: London, 1986.
(39) Wagman, D. D.; Evans, W. H. E.; Parker, V. B.; Schum, R. H.; Halow, I.; Mailey, S. M.; Churney, K. L.; Nuttall, R. L. The NBS Tables of Chemical Thermodynamic Properties. *J. Phys. Chem. Ref. Data* **1982**, *11* (Suppl. 2).
(40) Smith, B. J.; Radom, L. *Chem. Phys. Lett.* **1994**, *231*, 345−351.
(41) Smith, B. J.; Radom, L. *J. Phys. Chem.* **1995**, *99*, 6468−6471.
(42) Herzberg, G. *Molecular Spectra and Molecular Structure II. Infrared and Raman Spectra of Polyatomic Molecules*; D. Van Nostrand Co. Inc.: Princeton, 1945.
(43) Cox, J. D.; Wagman, D. D.; Medvedev, V. A. *CODATA Key Values for Thermodynamics*; Hemisphere Publishing Corp.: New York, 1989.
(44) Chupka, W. A.; Berkowitz, J. *J. Chem. Phys.* **1967**, *47*, 2921−2933.